第 24 卷第 2 期 无 机 化 学 学 报 Vol.24 No.2
2008 年 2 月 CHINESE JOURNAL OF INORGANIC CHEMISTRY 181~190

碳包覆 $Li_3V_2(PO_4)_3$:溶胶-凝胶法合成及性能

陈权启[1,2] 何伟春[1,3] 王建明*,[1] 唐 征[1] 邵海波[1] 张鉴清[1,4]
([1]浙江大学化学系,杭州 310027)
([2]湘潭大学化学学院,湘潭 411105)
([3]河南工业大学材料科学与工程学院,郑州 450007)
([4]中国金属腐蚀与防护国家重点实验室,沈阳 110015)

摘要:利用 V_2O_5、$LiOH\cdot H_2O$、H_2O_2、$NH_4H_2PO_4$ 与柠檬酸为原料,通过溶胶-凝胶法合成了碳包覆的 $Li_3V_2(PO_4)_3$ 复合正极材料。采用 XPS、XRD、SEM、TEM、拉曼光谱和电化学方法对材料的性能进行了研究。还研究了其结构与焙烧温度、样品电导率和电化学性能的关系。研究表明复合材料具有空间群为 $P2_1/n$ 的单斜结构,表面包覆粗糙多孔的碳层。在 800 ℃下制备的碳包覆样品的电子导电率高达 9.81×10^{-5} S·cm^{-1},约为高温固相氢气还原法制备的未包覆碳 $Li_3V_2(PO_4)_3$ 的 10000 倍。测试结果表明碳包覆 $Li_3V_2(PO_4)_3$ 的电化学性能远优于未包覆碳的样品。在 3.0~4.3 V 电压范围内,以 0.1C 和 2C 倍率充放电时,碳包覆的 $Li_3V_2(PO_4)_3$ 具有高比容量(分别为 128 和 109 mAh·g^{-1})和优异的循环性能。

关键词:磷酸钒锂;溶胶凝胶法;碳包覆;锂离子电池
中图分类号:O614.111; O614.81; TM912.9 **文献标识码**:A **文章编号**:1001-4861(2008)02-0181-10

Carbon-coated $Li_3V_2(PO_4)_3$ Composite Cathode Material for Lithium-ion Batteries: Sol-gel Synthesis and Performance

CHEN Quan-Qi[1,2] HE Wei-Chun[1,3] WANG Jian-Ming*,[1] TANG Zheng[1]
SHAO Hai-Bo[1] ZHANG Jian-Qing[1,4]
([1]*Department of Chemistry, Zhejiang University, Hangzhou* 310027)
([2]*College of Chemistry, Xiangtan University, Xiangtan, Hunan* 411105)
([3]*College of Material Science and Engineering, Henan University of Technology, Zhengzhou* 450007)
([4]*State Key Laboratory for Corrosion and Protection, Chinese Academy of science, Shenyang* 110015)

Abstract: A carbon-coated $Li_3V_2(PO_4)_3$ composite cathode material was synthesized by a sol-gel method using V_2O_5, $LiOH\cdot H_2O$, H_2O_2, $NH_4H_2PO_4$ and citric acid as starting materials. Properties of the prepared composite material were investigated using XPS, XRD, SEM, Raman spectroscopy, TEM, and various electrochemical techniques. The relationship among structure, calcination temperature, electronic conductivity and the electrochemical performance of samples was also studied. The sample obtained had a monoclinic structure with a space group of $P2_1/n$ and a rough and porous carbon surface layer. The electronic conductivity of the carbon-coated $Li_3V_2(PO_4)_3$ samples synthesized at 800 ℃ was about a factor of ~10^4 higher than that of carbon-free $Li_3V_2(PO_4)_3$ prepared by solid-state hydrogen reducing reaction. The results show that the carbon-coated $Li_3V_2(PO_4)_3$ is superior in the electrochemical performance to the carbon-free sample. In the voltage range of 3.0~4.3 V, the carbon-coated $Li_3V_2(PO_4)_3$ synthesized at 800 ℃ displays large reversible capacities (128 mAh·g^{-1} at 0.1C and 109 mAh·g^{-1} at 2C, respectively) and excellent cyclic stability. The reason for the excellent electrochemical performance of the carbon coated $Li_3V_2(PO_4)_3$ is discussed.

Key words: $Li_3V_2(PO_4)_3$; sol-gel method; carbon-coated; lithium-ion batteries

收稿日期:2007-09-13。收修改稿日期:2007-11-18。
国家自然科学基金(No.50172041)资助项目。
*通讯联系人。E-mail:wjm@zju.edu.cn
第一作者:陈权启,男,34 岁,博士研究生;研究方向:化学电源与功能材料。

Lithium ion batteries are attractive for portable devices due to their high operating voltage, large energy density, low self-discharge rate and long cycle life. Commercial lithium ion batteries widely use the layered $LiCoO_2$ cathode at present, but cobalt is expensive and relatively toxic. In recent years, much effort has been devoted to searching for new cathode materials in place of commercial cathode materials based on $LiCoO_2$ [1~5]. Monoclinic $Li_3V_2(PO_4)_3$, one kind of framework material based on the phosphate polyanion, has received intensive attention because of its stable framework, higher operating voltage than the counterpart oxides, good lithium ion transport and large theoretical capacity (133 and 197 mAh·g^{-1}, corresponding to cycling two lithium ions and all three lithium ions, respectively) [6~17]. However, pristine $Li_3V_2(PO_4)_3$ was considered to be a cathode material with intrinsic low electronic conductivity [7], and the low electronic conductivity degrades its electrochemical performance. Some previous reports have demonstrated that it is an effective method to improve the electrochemical performance of the cathode material with low electronic conductivity by enhancing its electronic conductivity[18~22]. The solutions to improving the electronic conductivity mainly include adding conductive materials, coating particles with a thin carbon layer and doping heteroatoms.

In the most of previous reports, $Li_3V_2(PO_4)_3$ had been prepared by solid-state techniques using hydrogen or carbon as reduction agents[6~12]. However, this synthesis process needs high calcination temperature and long sintering time [6~11], and it also requires several iterations between mixing and sintering to improve the homogeneity of the final products. These repeated heat treatments induce growth and aggregation of $Li_3V_2(PO_4)_3$, which adversely influences the electrochemical performance of the prepared $Li_3V_2(PO_4)_3$. Recently, $Li_3V_2(PO_4)_3$/carbon composites have been successfully prepared by a sol-gel method using V_2O_5 gel as vanadium sources and carbon gel or high surface carbon powder as reductant [14,15]. Nevertheless, in the two previous sol-gel methods, it took longer time to prepare the V_2O_5 gel, and the physical mixture of the raw materials could result in unevenness in the composition of the $Li_3V_2(PO_4)_3$/carbon composites.

In this paper, the carbon-coated $Li_3V_2(PO_4)_3$ samples have been synthesized by a sol-gel method using citric acid as the carbon sources for reduction and coating as well as a chelating agent, and the physical properties and electrochemical performance of the samples are investigated.

1 Experimental

1.1 Synthesis of $Li_3V_2(PO_4)_3$

The preparation of precursor gel was similar to our previous report[16]. 8 g V_2O_5 powder (supplied by Aldrich) was dissolved by slowly adding 300 mL of 10% (*V*/*V*) H_2O_2 solution with vigorous stirring for 2 h to get a clear orange solution, then citric acid equivalent molar to V_2O_5 and stoichiometric amounts of $NH_4H_2PO_4$ and $LiOH \cdot H_2O$ were added to the above orange solution. The mixed solution was aged with stirring at 60 ℃ for 10 h to obtain the green precursor gel. The obtained green gel was dried in a vacuum oven at 80 ℃, pelletized and heated at 300 ℃ in a tubular furnace with flowing argon gas at a flow rate of 150 sccm (standard cubic centimeter per minute) for 4 h to allow the evolution of NH_3 and H_2O. The resulting product was ground and pelletized again, and heated to 600~850 ℃ at a rate of 2 ℃·min^{-1} and kept for 8 h with a stream of argon gas (150 sccm). The carbon-coated $Li_3V_2(PO_4)_3$ composite sample was obtained through the above experimental procedure and is referred as CC-LVP (carbon-coated lithium vanadium phosphate) in this paper. For comparison, carbon-free $Li_3V_2(PO_4)_3$ sample, referred as CF-LVP (carbon-free lithium vanadium phosphate) in this paper, was prepared through solid-state hydrogen reducing reaction using V_2O_5, $NH_4H_2PO_4$ and Li_2CO_3 as starting materials and hydrogen as reductant for V_2O_5 according to reference[6].

During the synthesis of $Li_3V_2(PO_4)_3$ composite, citric acid as a chelating agent for vanadium facilitates the formation of the homogenous precursor gel; moreover, its decomposition at higher temperatures in an inert atmosphere[23,24] may provide the well-dispersed carbon that was used as the selective reduction agent for V(Ⅴ) and the coating material for $Li_3V_2(PO_4)_3$[8].

1.2 Physical characterization

Thermogravimetric (TG) analysis and differential scanning calorimetry (DSC) were carried out using NETZSCHSTA 409 PG/PC thermal analyzer heating from room temperature to 950 ℃ (10 ℃·min^{-1}) in N_2 atmosphere. The structures of the samples were characterized by a D/Max Ⅲ X-ray diffractometer (Rigaku, Japan) with Ni filtered Cu $K\alpha$ radiation (λ = 0.154 18 nm) at 40 kV and 300 mA, and the scan rate (2θ) of 8°·min^{-1} was applied to record the pattern in the 2θ range of 10°~80° by means of scintillation detector. The surface morphology of the samples was observed using a SIRION-100 (FEI, USA) scanning electron microscopy (SEM) with an accelerating voltage of 10~20 kV and the maximum current of 230 μA. The microstructure was examined using a JEM 1010 (JEOL, Japan) transmission electron microscope (TEM) with an accelerating voltage of 100 kV. Before observation, the samples were dispersed in anhydrous ethanol by ultrasonic agitation, and the suspension solution was dropped onto a standard copper TEM grid. The valences of vanadium in dried gel and $Li_3V_2(PO_4)_3$ were examined by a Thermo ESCALAB (Thermo VG scientific,UK) X-ray photoelectron spectroscopy (XPS) with monochromatic Al $K\alpha$ radiation (1486.6 eV). The pressure in the chamber was about 1.0×10^{-8} Pa. The C1s line of adventious carbon at 285.0 eV was used as internal standard to calibrate the binding energies. The carbon content of samples was determined by a carbon-sulfur analyser (Mlti EA2000). The Raman spectra of the carbon-coated $Li_3V_2(PO_4)_3$ composites prepared at different temperatures were measured with a Jobin-Yvon U1000 double pass spectrometer (Longjumeau, France) and the incident light used for experiments was the 515.4 nm Ar line of a laser source. The electronic conductivity of samples was determined by a direct volt-ampere method on disc samples prepared by pressing about 1.5 g $Li_3V_2(PO_4)_3$ powders up to 30 MPa in module. The top and bottom surfaces of the discs were coated with gold by Fine Coat Ion Sputter JFC-1100 (JEOL, Japan). The conductivity measurements of disc samples were carried out on Potentiosta/Gavansta Model 273A(EG&G, USA) by linear sweep voltammetry between 0 and 100 mV at a scan rate of 0.1 mV·s^{-1} with each increment of 10 mV. The electronic conductivity, σ, is calculated by the formula of $\sigma=\frac{4h}{\pi d^2}k$, where h and d is the thickness (~5 mm) and the diameter(~12 mm) of disc samples, respectively, and k is the slope of the *I-E* curves.

1.3 Electrochemical test

The electrochemical tests of the samples were carried out using two-electrode or three-electrode cells. In all cells, lithium metal was served as counter and reference electrodes, Celguard-2300 was used as separator, and the electrolyte was 1mol·L^{-1} $LiPF_6$ solution in a mixture of ethylene carbonate/dimethyl carbonate (1∶1 *V*/*V*). The CC-LVP and CF-LVP cathodes were prepared by coating a slurry of 80% CC-LVP, 10% carbon black and 10% poly(vinylidene difluoride), and a slurry of 75% CF-LVP, 15% carbon black and 10% poly (vinylidene difluoride), respectively, on aluminium foil current collector. After dried at 120 ℃ in a vacuum oven for 24 h, the resulting electrodes with an active material loading of about 8 mg·cm^{-2} were transferred to an Ar-filled glove box to assemble testing cells. Galvanostatic charge-discharge measurements were carried out in two-electrode cells using a PCBT-138-320 battery programme-control test system (Lixing, Wuhan, China). Cyclic voltammetry (CV) was conducted in three-electrode cells at a scan rate of 0.05 mV·s^{-1} by Potentiosta/Gavansta Model 273A.

2 Results and discussion

Fig.1 shows the TG-DSC curves of the dried precursor gel. On the DSC curve near 132 ℃, there is an obvious endothermic peak, associating with the sharp weight loss on the TG curve, which is related to the fast dehydration of precursor gel. There is a broad exothermic peak near 518 ℃ on the DSC curve, possibly associating with evolution of NH_3 and H_2O, decomposition of organic compound and formation of $Li_3V_2(PO_4)_3$. When the temperature is higher than 600 ℃, TG curve shows that the weight almost remains constant, implying that the formation of $Li_3V_2(PO_4)_3$ phase begins at this temperature. Based on the above analysis, the

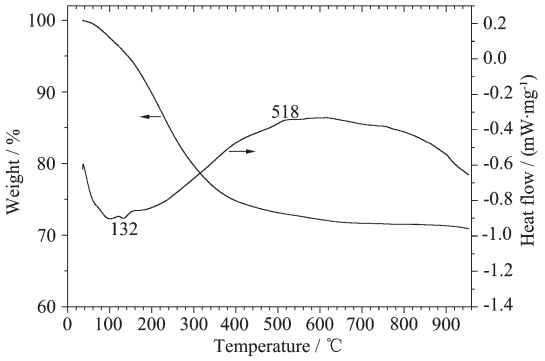

Fig.1 TG-DSC curves of the precursor gel

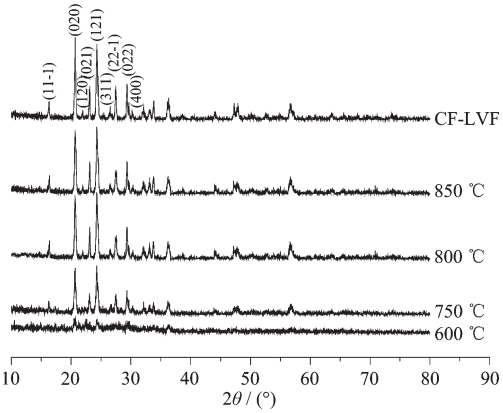

Fig.2 XRD patterns of carbon-free sample and samples prepared at different temperatures by sol-gel method

calcination temperature for the dried precursor gel is adjusted in the range of 600~850 ℃.

The XRD patterns of various $Li_3V_2(PO_4)_3$ samples are shown in Fig.2. It can be seen that the XRD patterns of all samples except for the sample calcined at 600 ℃ are in good agreement with that of monoclinic $Li_3Fe_2(PO_4)_3$ (PDF 43-0526). The unit cell parameters obtained from the least square refinement based on a monoclinic structure using space group $P2_1/n$ are listed in Table 1. When the calcination temperature is 600 ℃, monoclinic $Li_3V_2(PO_4)_3$ appears, but its diffraction intensity is very weak and impurity phases are observed. The diffraction intensity of the samples increases with increasing calcination temperature, suggesting that higher temperatures are beneficial for the improvement of $Li_3V_2(PO_4)_3$ crystallinity. The CC-LVP samples display smaller crystal cell sizes than CF-LVP, which could result from the inhibition of the well-dispersed carbon originated from the decomposition of citric complexes for the growth of $Li_3V_2(PO_4)_3$ crystals. This may suggest that the electrochemical performance of CC-LVP is better than that of CF-LVP.

Table 1 Lattice parameters of $Li_3V_2(PO_4)_3$ samples synthesized at different conditions

Sample	Preparation conditions	a / nm	b / nm	c / nm	β / (°)	V / nm^3
CC-LVP	dried gel calcined at 750 ℃	0.861 7	0.861 0	1.206 3	90.64	0.894 9
CC-LVP	dried gel calcined at 800 ℃	0.862 0	0.860 9	1.206 1	90.57	0.895 0
CC-LVP	dried gel calcined at 850 ℃	0.861 6	0.861 6	1.206 4	90.60	0.895 5
CF-LVP	solid state reaction using hydrogen as reductant for V_2O_5	0.864 8	0.862 1	1.208 0	90.46	0.900 6

Typical SEM images for the CC-LVP samples prepared at 750, 800 and 850 ℃ and CF-LVP are presented in Fig.3. The CC-LVP samples display smaller particle size than CF-LVP, and the particle size and crystalinity of the CC-LVP samples increase with increasing calcination temperature. It can be seen that the CC-LVP sample prepared at 800 ℃ shows relatively small and uniform particle size, porous structure and good crystallinity, implying that it could have better electrochemical performance. Fig.4 illustrates that the

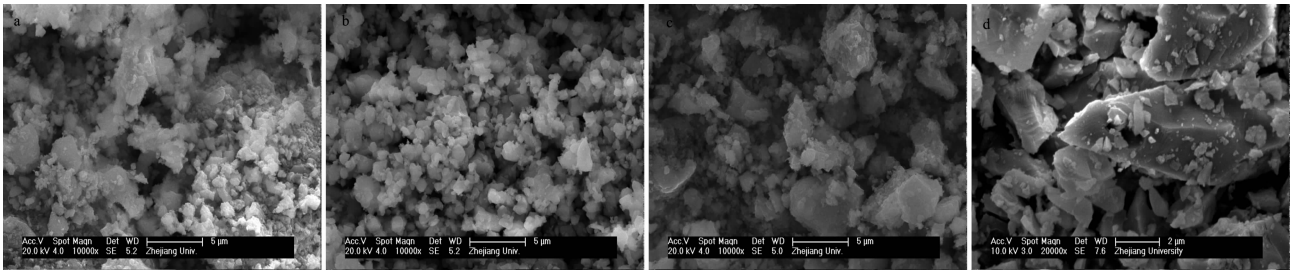

Fig.3 SEM images of CC-LVP calcined at (a) 750 ℃; (b) 800 ℃; (c) 850 ℃ and CF-LVP (d)

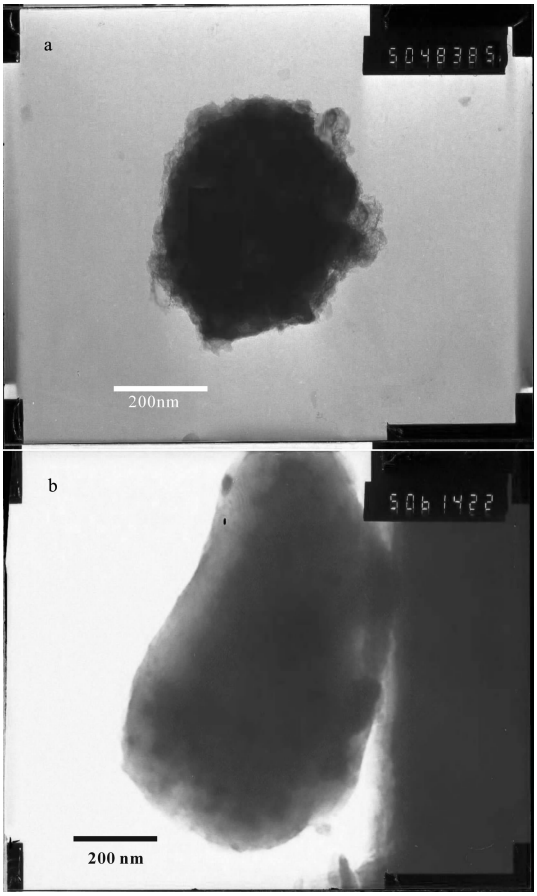

Fig.4　TEM images of the CC-LVP synthesized at 800 ℃ (a) and CF-LVP (b)

TEM images of the CC-LVP sample prepared at 800 ℃ and CF-LVP. The CF-LVP sample particles exhibit smooth surfaces. Whereas the CC-LVP sample displays a particle size of about 400 nm, and its particle surfaces are covered with a porous nanostructured carbon layer. The existence of the thin porous carbon layer may enhance the electronic conductivity and inhibit the growth of particle.

The XPS spectra of the dried gel and CC-LVP are shown in Fig.5. The absence of N peak in the XPS of CC-LVP and the presence of C peak in the XPS of both samples indicate the complete decomposition of $NH_4H_2PO_4$ and the existence of residual carbon in the final product. The inset in Fig.5 shows that the binding energy for V2$p_{3/2}$ peak of the dried gel (515.7 eV) is higher than that for the corresponding peak of CC-LVP (515.2 eV), suggesting that the valence of vanadium in the dried gel is higher than that in CC-LVP. It can be concluded from previous results [25,26] that the valence

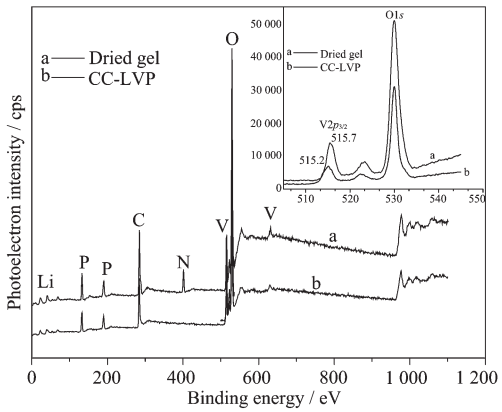

Fig.5　XPS spectra of the dried precursor gel and the CC-LVP calcined at 800 ℃. The inset shows V2p spectra of the corresponding samples

state of vanadium in the gel and $Li_3V_2(PO_4)_3$ is +4 and +3, respectively. The transfer of V^{5+} to V^{4+} may originate from the reduction effect of H_2O_2 and citric acid on V_2O_5. While in the previous reports [14,15], the valence state of vanadium in the gel precursors could be +5 due to the absence of an effective reductant. The relatively lower valence state (+4) of vanadium in our gel precursor may be partially responsible for the lower calcination temperature and shorter reaction time during synthesis of CC-LVP. In addition, the addition of H_2O_2 and citric acid may have significant contribution to fast formation of the gel precursor.

Raman spectroscopy is a particularly useful tool for characterizing the carbon films because carbon is a relatively strong scatterer with two Raman-active E_{2g} modes. Fig.6 shows the Raman spectra of CC-LVP samples prepared at 600~850 ℃ and the deconvolution for the Raman spectrum of the CC-LVP prepared at 600 ℃ using a fit with four Gaussian bands. Two intense and broad bands at about 1 372 and 1 594 cm^{-1} in all the CC-LVP samples are assigned to the D and G bands of the residual carbon, respectively. The intensity of D and G bands decreases with increasing calcination temperature, which could result from the decrease of carbon content at higher temperatures. To resolve the Raman spectra of the residual carbon, a standard peak deconvolution procedure after polynomial background subtraction was applied. A deconvolution of all the Raman spectra using a fit with D and G lines did not give accurate results. Four Gaussian bands are

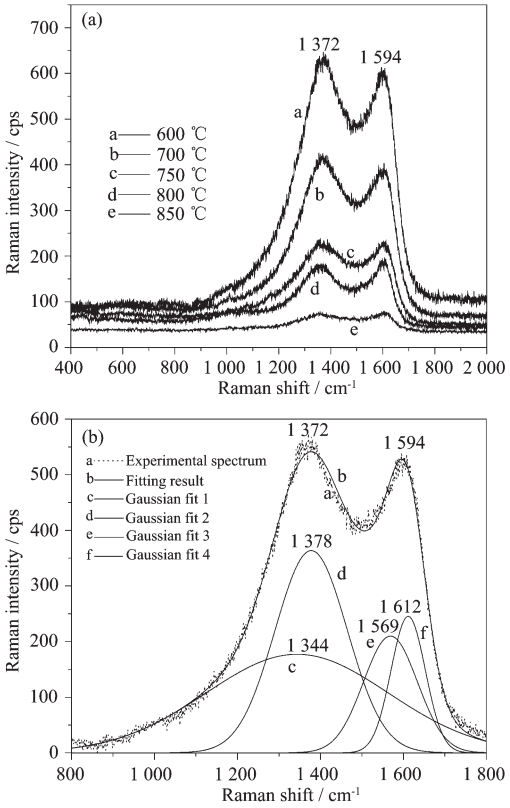

Fig.6 (a) Raman spectra of CC-LVP prepared at different temperatures. (b) Raman spectrum of the residual carbon in the CC-LVP prepared at 600 ℃ and its fitting result

necessary to account for the observed Raman features with minimum error. The corresponding bands are at about 1 344, 1 378, 1 569 and 1 612 cm^{-1}, respectively. The bands at 1 344 and 1 569 cm^{-1} are assigned to sp^2 graphite-like structure with relatively good electronic conductivity, and the two others originate from the sp^3 type often observed in amorphous carbonaceous material[27,28]. The ratio of sp^2 to sp^3 is defined as the integral of the Gaussians ($I_{1344}+I_{1569}$) to ($I_{1378}+I_{1612}$) in Fig. 6b. The same deconvolution procedure was applied to the Raman spectra of all the CC-LVP samples, and the results of sp^2/sp^3 for samples synthesized at 600, 700, 750, 800 and 850 ℃ are 1.26, 1.20, 1.71, 2.06 and 1.98, respectively. The results show that higher calcination temperature facilitates the increase of the sp^2 structure fraction in residual carbon. This implies that the CC-LVP samples prepared at higher temperatures have higher electronic conductivity[29].

The *I-E* curves for the different tested disc $Li_3V_2(PO_4)_3$ samples measured by linear sweep voltammetry are presented in Fig.7. The slope, k, is obtained from the *I-E* curves, then the conductivity, σ, is calculated by the formula $\sigma = \frac{4h}{\pi d^2}k$. The results of electronic conductivity of various $Li_3V_2(PO_4)_3$ samples are listed in Table 2. All CC-LVP samples display much higher electronic conductivity than CF-LVP because of the existence of the carbon coating layer. With increasing calcination temperature, the electronic conductivity of CC-LVP increases although carbon content decreases as shown in Table 2. This may result from the increase of the sp^2 structure fraction in the carbon coating layer of CC-LVP with increasing calcination temperature. The electronic conductivity of the CC-LVP samples synthesized at 800 and 850 ℃ is 9.81×10^{-5} and 1.14×10^{-4} $S\cdot cm^{-1}$, respectively, about a factor of ~10^4 higher than that of CF-LVP.

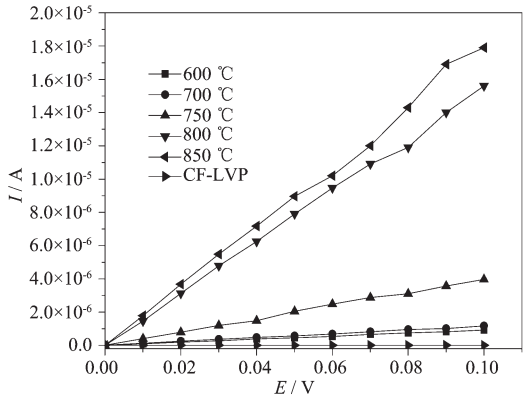

Fig.7 *I-E* plots for $Li_3V_2(PO_4)_3$ samples prepared at different conditions

Table 2 Electronic conductivity and carbon content of $Li_3V_2(PO_4)_3$ samples

Sample	Carbon content / wt%	σ / ($S\cdot cm^{-1}$)
Calcination at 600 ℃ for 8 h	6.25	5.88×10^{-6}
Calcination at 700 ℃ for 8 h	4.80	7.26×10^{-6}
Calcination at 750 ℃ for 8 h	4.25	2.53×10^{-5}
Calcination at 800 ℃ for 8 h	3.15	9.81×10^{-5}
Calcination at 850 ℃ for 8 h	2.85	1.14×10^{-4}
Solid state hydrogen reduction at 850 ℃ for 16 h	0	7.52×10^{-9}

Fig.8 shows the initial charge-discharge profiles of CC-LVP samples prepared at different temperatures and CF-LVP at 0.1C (13.3 $mA\cdot g^{-1}$) in the voltage range

of 3.0~4.3 V at 25 ℃. Fig.9 reveals that the effects of calcination temperature on the capacity and electronic conductivity of CC-LVP and CF-LVP. It is clear that the capacity of CC-LVP samples increases with increasing calcination temperature from 600 to 800 ℃, consistent with the variation trend of electronic conductivity with calcination temperature. The CC-LVP sample prepared at 850 ℃ displays relatively lower reversible capacity than the CC-LVP sample synthesized at 800 ℃ although it has higher electronic conductivity than other samples, resulting from its larger particle size due to agglomeration. All $Li_3V_2(PO_4)_3$ samples except for the CC-LVP prepared at 600 ℃ exhibit three charge plateaus and the corresponding three discharge plateaus, corresponding to three compositional regions of $Li_{3-x}V_2(PO_4)_3$, that is, x=0.0~0.5, x=0.5~1.0 and x=1.0~2.0[6,7]. The lower crystallinity and impurities may be mainly responsible for the smaller reversible capacities of CC-LVP calcined at relatively low temperatures (600 and 700 ℃). The CC-LVP samples synthesized at 750, 800 and 850 ℃ present lower charge voltage plateau and higher discharge voltage plateau than CF-LVP, indicating that these CC-LVP samples have smaller electrode polarization due to their larger electronic conductivities. It is noted that among all the tested samples the CC-LVP prepared at 800 ℃ displays the highest discharge potential plateaus and the largest reversible capacity 128 mAh·g^{-1}, nearly equivalent to the reversible cycling of two lithium ions per $Li_3V_2(PO_4)_3$ formula unit (133 mAh·g^{-1}). The cyclic performance of CC-LVP prepared at different temperatures and CF-LVP at 0.1C in the voltage range of 3.0~4.3 V at 25 ℃ is shown in Fig.10. All the tested samples present a large capacity retention rate (>95%) after 30 cycles, suggesting their better electrochemical-cycling under the present experimental conditions. The sequence of reversible capacity is CC-LVP at 800 ℃> CC-LVP at 850 ℃>CC-LVP at 750 ℃>CF-LVP>CC-LVP at 700 ℃>CC-LVP at 600 ℃, consistent with the corresponding initial capacity sequence shown in Fig.8.

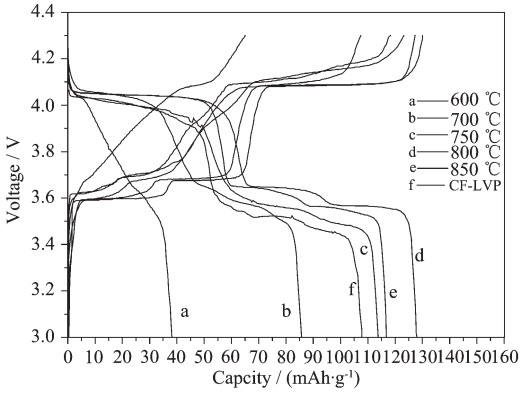

Fig.8　Initial charge-discharge profiles of CC-LVP samples calcined at different temperatures and CF-LVP at 0.1 C in the voltage range of 3.0~4.3V at 25 ℃

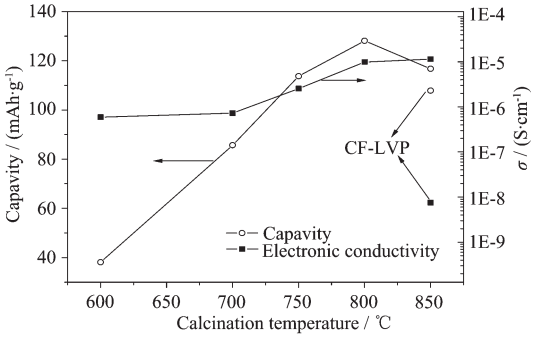

Fig.9　Variation in the capacity and electronic conductivity of CF-LVP and CC-LVP with calcination temperature

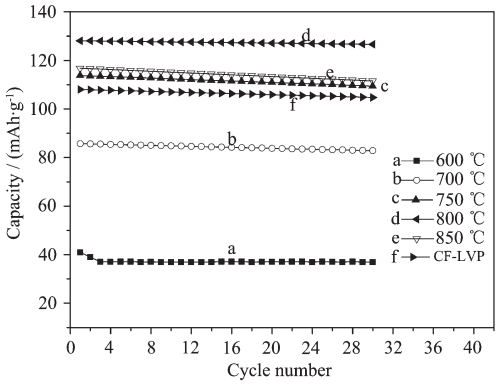

Fig.10　cycle performance of CF-LVP and CC-LVP samples prepared at different temperatures at 0.1C in the voltage range of 3.0~4.3 V at 25 ℃

Fig.11 and 12 show the initial charge-discharge profiles and cyclic performance of CC-LVP and CF-LVP samples at 2C in the voltage range of 3.0~4.3 V at 25 ℃, respectively. The CF-LVP sample displays larger electrode polarization and much smaller reversible capacity than CC-LVP at 2C, which may result from the very low electronic conductivity of CF-LVP. The

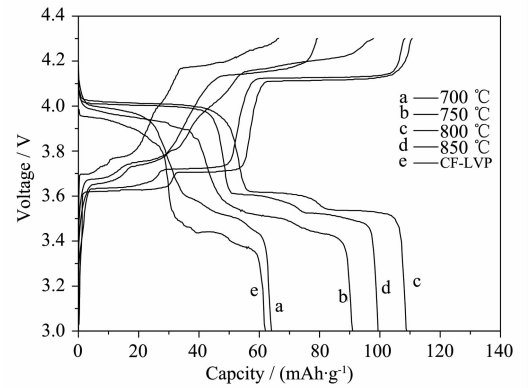

Fig.11 Initial charge-discharge profiles of CF-LVP and CC-LVP samples prepared at different temperatures at 2C in the voltage range of 3.0~4.3 V at 25 ℃

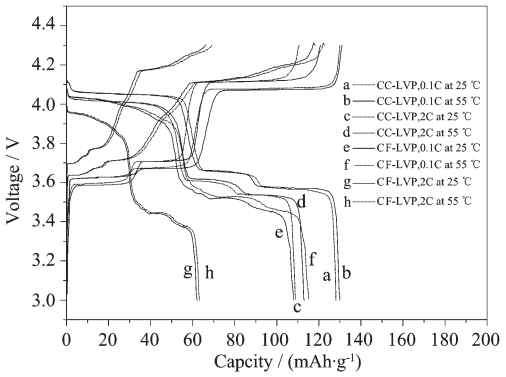

Fig.13 Initial charge-discharge profiles of CF-LVP and CC-LVP prepared at 800 ℃ at 0.1 C and 2C in the voltage range of 3.0~4.3 V at 25 and 55 ℃

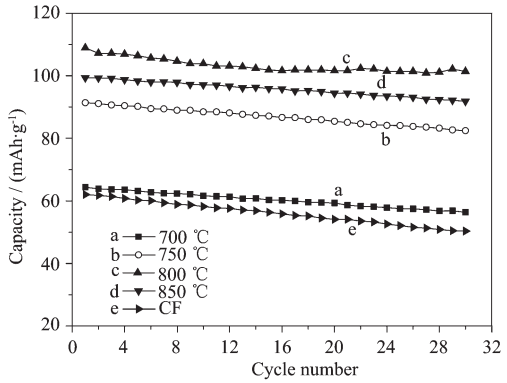

Fig.12 Cyclic performance of CF-LVP and CC-LVP samples prepared at different temperatures at 2C in the voltage range of 3.0~4.3 V at 25 ℃

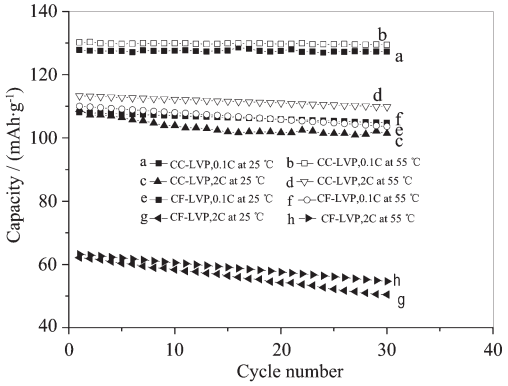

Fig.14 Cyclic performance of CF-LVP and CC-LVP prepared at 800 ℃ at 0.1C and 2C in the voltage range of 3.0~4.3 V at 25 and 55 ℃

comparison of the data in Fig.8 and 11 indicates that the variation trend in reversible capacity of CC-LVP with calcination temperature at 2C is in general agreement with that at 0.1C, but the capacity value at 2C is lower than that at 0.1C. It can also be seen from Fig.10 and 12 that the CF-LVP sample show relatively lower cyclic stability at 2C than at 0.1C. These may result from larger electrode polarization and poor structure stability of CF-LVP at a higher charge-discharge rate.

In order to investigate the effects of test temperature on the electrochemical performance of $Li_3V_2(PO_4)_3$, the CC-LVP prepared at 800 ℃ and CF-LVP were cycled at 0.1 and 2C in the voltage range of 3.0~4.3 V at 25 and 55 ℃, respectively, and the results are shown in Fig.13 and 14. Fig.13 shows that the initial electrochemical performance of the two samples is enhanced at the elevated temperature. This mainly results from the improved lithium ion diffusion at the elevated temperature[30~32]. At 55 ℃, the capacity of CC-LVP is 130 mAh·g^{-1} at 0.1C, very close to the theoretical capacity of 133 mAh·g^{-1}, and the capacity is 113 mAh·g^{-1} at 2C. For CF-LVP, the capacity increase at 0.1C is higher (from 108 at 25 ℃ to 115 at 55 ℃) than that at 2C (from 62 at 25 ℃ to 63.3 at 55 ℃). While the capacity increase of CC-LVP is higher at low rate. The different trend of increase may mainly result from the different increment of lithium ion diffusion coefficient of CF-LVP and CC-LVP samples. The increment of lithium ion diffusion coefficient of CC-LVP is much higher than that of CF-LVP, so the capacity increase of CC-LVP is higher than that of CF-LVP at 2C. While the increase of capacity of CF-LVP is higher than that of CC-LVP at 0.1C, the reason for that

is that the capacity of CC-LVP is very close to the theoretical capacity, it is difficult to increase capacity significantly. The decrease in the electrochemical performance of the samples at larger charge-discharge rate, as before, is due to the increase of electrode polarization. It can be seen from Fig.14 that the two samples show excellent cyclic performance in the voltage range of 3.0~4.3 V at the elevated temperature, especially at lower charge-discharge rate.

Cyclic voltammetry (CV) measurement was carried out in the voltage range of 3.0 ~4.3 V to further understand the charge-discharge behaviour of the $Li_3V_2(PO_4)_3$ electrode, and the results are shown in Fig.15. Three oxidation peaks and three corresponding reduction ones occur on the CV curve in the voltage range of 3.0~4.3 V, consistent with the existence of three pairs of charge-discharge plateaus in Fig.8. All the oxidation and reduction peaks are associated with the V^{3+}/V^{4+} couple[6,7]. The first, second and third oxidation peaks correspond to the extraction of lithium reaction, $Li_3V_2(PO_4)_3 \rightarrow Li_{2.5}V_2(PO_4)_3$, $Li_{2.5}V_2(PO_4)_3 \rightarrow Li_2V_2(PO_4)_3$ and $Li_2V_2(PO_4)_3 \rightarrow LiV_2(PO_4)_3$, respectively. The corresponding reduction peaks are associated with the lithium insertion reaction, $LiV_2(PO_4)_3 \rightarrow Li_2V_2(PO_4)_3$, $Li_2V_2(PO_4)_3 \rightarrow Li_{2.5}V_2(PO_4)_3$ and $Li_{2.5}V_2(PO_4)_3 \rightarrow Li_3V_2(PO_4)_3$, respectively. It can be seen from Fig.15 that the CV curves for CC-LVP show lower oxidation peak potential and higher reduction peak potential than those for CF-LVP, implying smaller electrode polarization for CC-LVP. This agrees well with the results of the charge-discharge experiments.

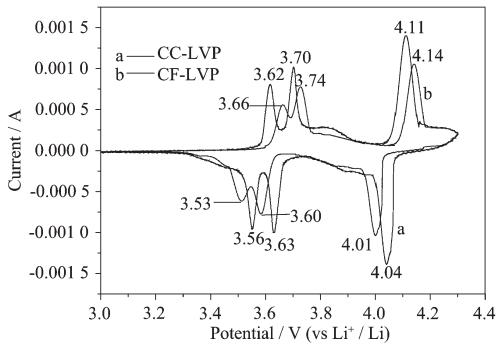

Fig.15　Cyclic voltamograms for the CC-LVP and CF-LVP electrodes at a scanning rate of 0.05 $mV \cdot s^{-1}$ in the voltage range of 3.0~4.3 V at 25 ℃

3　Conclusions

The carbon-coated $Li_3V_2(PO_4)_3$ samples have been synthesized by a sol-gel method using citric acid as both a chelating agent and carbon source. The single-phase $Li_3V_2(PO_4)_3$ obtained by calcination of the precursor gel at 800 and 850 ℃ shows a monoclinic structure with a space group of $P2_1/n$, and the $Li_3V_2(PO_4)_3$ particles are covered with a rough and porous carbon layer. With increasing calcination temperature, the sp^2/sp^3 value in the coated carbon layer increases, and results in the improvement for the electronic conductivity of CC-LVP. The electronic conductivity of the CC-LVP samples synthesized at 800 and 850 ℃ is about a factor of $\sim 10^4$ higher than that of the carbon-free $Li_3V_2(PO_4)_3$ synthesized by solid state hydrogen reducing reaction. The carbon-coated $Li_3V_2(PO_4)_3$ samples show smaller electrode polarization than CF-LVP due to the improved electronic conductivities, thus their electrochemical performance is obviously enhanced. The CC-LVP samples calcined at higher temperatures (800 and 850 ℃) display much better electrochemical performance than CC-LVP calcined at lower temperatures (600 and 700 ℃), consistent with the variation trend of electronic conductivity with calcination temperature. The elevated test temperature may enhance the electrochemical performance of $Li_3V_2(PO_4)_3$ samples. Among all the tested samples the CC-LVP prepared at 800 ℃ displays the highest discharge potential plateaus and the largest reversible capacity. Small particle size, porous carbon coating layer and relatively high electronic conductivity may be responsible for its excellent electrochemical performance.

References:

[1] Ohzuku T, Ueda A, Nagayama M, et al. *J. Electrochem. Soc.*, **1993**,**140**(7):1862~1870

[2] LI Yi-Bing(李义兵), CHEN Bai-Zhen(陈白珍), HU Yong-Jun(胡拥军), et al. *Chinese J. Inorg. Chem.* (*Wuji Huaxue Xuebao*), **2006**,**22**(6):983~987

[3] FANG Hai-Sheng(方海升), WANG Zhi-Xing(王志兴), LI Xin-Hai(李新海), et al. *Chinese J. Inorg. Chem.* (*Wuji Huaxue Xuebao*), **2006**,**22**(2):311~315

[4] LIU Xin-Yan(刘欣艳), XIA Ding-Guo(夏定国), ZHAO Yu-Juan(赵煜娟), et al. *Chinese J. Inorg. Chem.* (*Wuji Huaxue Xuebao*), **2006**,**22**(2):321~325

[5] ZHANG Jing(张 静), LIU Su-Qin(刘素琴), HUANG Ke-Long(黄可龙), et al. *Chinese J. Inorg. Chem.* (*Wuji Huaxue Xuebao*), **2005**,**21**(3):433~436

[6] Saidi M Y, Barker J, Huang H, et al. *J. Power Sources*, **2003**, **119-121**:266~272

[7] Yin S C, Grondey H, Strobel P, et al. *J. Am. Chem. Soc*., **2003**,**125**(34):10402~10411

[8] Barker J, Saidi M Y, Swoyer J L, et al. *J. Electrochem. Soc*., **2003**,**150**(6):A684~A688

[9] Gaubicher J, Wurm C, Goward G, et al. *Chem. Mater.*, **2000**, **12**(11):3240~3242

[10]Fu P, Zhao Y M, Dong Y Z, et al. *J. Power Sources*, **2006**, **162**(1):651~657

[11]Ren M M, Zhou Z, Li Y Z, et al. *J. Power Sources*, **2006**, **162**(2):1357~1362

[12]Fu P, Zhao Y M, Dong Y Z, et al. *Electrochim. Acta*, **2006**, **52**(3):1003~1008

[13]LIU Su-Qin(刘素琴), LI Shi-Cai (李世彩),TANG Lian-Xing (唐联兴),et al. *Chinese J. Inorg. Chem.* (*Wuji Huaxue Xuebao*), **2006**,**22**(4):645~650

[14]Huang H, Yin S C, Kerr T, et al. *Adv. Mater.*, **2002**,**14**(21): 1525~1528

[15]Li Y Z, Zhou Z, Ren M M, et al. *Electrochim. Acta*, **2006**, **51**(28):6498~6502

[16]Chen Q Q, Wang J M, Tang Z, et al. *Electrochim. Acta*, **2007**, **52**(16):5251~5257

[17]ZHONG Sheng-Kui(钟胜奎), YIN Zhou-Lan(尹周澜), WANG Zhi-Xing(王志兴), et al. *Chinese J. Inorg. Chem.*(*Wuji Huaxue Xuebao*), **2006**,**22**(10):1843~1846

[18]Teng T H, Yang M R, Wu S H, et al. *Solid State Commun*., **2007**,**142**(7):389~392

[19]Wolfenstine J, Read J, Allen J L. *J. Power sources*, **2006**, **163**(2):1070~1073

[20]Park K S, Son J T, Chung H T, et al. *Solid State Commun.*, **2004**,**129**(5):311~314

[21]Yang J, Xu J J. *J. Electrochem. Soc*., **2006**,**153**(4):A716~A723

[22]Sides C R, Croce F, Young V Y, et al. *Electrochem. Solid-state Lett.*, **2005**,**8**(9):A484~A487

[23]Dominko R, Bele M, Gaberscek M, et al. *J. Electrochem. Soc*., **2005**,**152**(3):A607~A610

[24]Hsu K F, Tsay S Y, Hwang B J, et al. *J. Mater. Chem*., **2004**, 14(17):2690~2695

[25]Mendialdua J, Casanova R, Barbaux Y, et al. *J. Electron. Spectrosc. Relat. Phenom.*, **1995**,**71**(3):249~261

[26]Silversmit G, Depla D, Poelman H, et al. *J. Electron. Spectrosc. Relat. Phenom.*, **2004**,**135**(2-3):167~175

[27]Kostecki R, Schnyder B, Alliata D, et al. *Thin Solid Films*, **2001**,**396**(1-2):36~43

[28]Salah A A, Mauger A, Zaghib K, et al. *J. Electrochem. Soc*., **2006**,**153**(9):A1692~A1701

[29]Wilcox J D, Doeff M M, Marcinek M, et al. *J. Electrochem. Soc*., **2007**,**154**(3):A389~A395

[30]Andersson A S, Thomas J O, Kalska B, et al. *Electrochem. Solid-State Lett*., **2000**,**3**(2):66~68

[31]Takahashi M, Tobishima S, Takei K, et al. *Solid State Ionics*, **2002**,**148**(3-4):283~289

[32]Wu S, Hsiao K, Liu W. *J. Power sources*, **2005**,**146**(1-2): 550~554